Victoria Yu. Salamatova, Alexandra S. Yurova, Yuri V. Vassilevski*, and Lin Wang

Automatic segmentation algorithms and personalized geometric modelling for a human knee

https://doi.org/10.1515/rnam-2019-0031
Received November 6, 2019; accepted November 8, 2019

Abstract: Human knee is one of the most complex joints. Different reasons may lead to knee instability. A personalized mathematical model of the knee may improve both diagnostic procedure and knee surgery outcomes. Such models require accurate geometric representation of bones and attachment sites of ligaments and tendons. This paper addresses automatic segmentation of knee bones and detection of origins and insertions for tendons and ligaments. The approach is based on anatomical features of bones and landmarks of tendons/ligaments attachments on the CT images. It provides a tool for the design of patient-specific geometrical knee models.

Keywords: Knee ligaments, knee tendons, bones segmentation, geometric model.

MSC 2010: 92C10, 68U10

Human knee is one of the most complex and commonly injured joints [5]. Different reasons may cause knee instability: ligaments weakness (laxity), local soft tissues injuries or even genetic factors [9]. Contemporary clinical examinations identify injured versus non-injured structures and determine the change in laxity of ligaments or muscles before and after a treatment. A personalized musculoskeletal model of the knee may improve the quality of clinical laxity assessments by estimation of key ligament stiffness and contact forces.

The conventional pipeline of mathematical modelling of a musculoskeletal system consists of the following stages: geometric model; biomechanical model of soft tissues (muscles, ligaments, cartilages) and bones; discretization of differential equations; numerical implementation and engineering analysis. The clinical task configures complexity and detalization of the model. For instance, addressing impact of patient-specific geometry of the joint requires an image-based geometrical model, addressing pathology of muscles requires a 3D model of tendon-muscle system etc.

Each personalized musculoskeletal knee model should be based on an adequate geometrical model. Clinical applications such as preoperative modelling of knee surgery or gait analysis, require accurate geometric representation of bones and detection of origins and insertions of ligaments and tendons. A geometrical model is a surface or volume mesh for bones composing the knee and sites of ligaments/tendons attachments. Such model is based on segmented patient-specific medical image which is conventionally given as a 3D array of voxels with intensity values in each voxel. Segmentation implies assigning or labeling every image voxel to a particular anatomical structure (tissue or organ). Manual segmentation is very time-consuming and developing automatic segmentation methods is the topical problem in biomedical engineering [7].

Automatic segmentation is based on conventional and universal features of medical images. Such universalism is immanent to CT rather than MRI images, and we segment CT data to provide a personalized geometric model of the knee. The origins and insertions of the knee ligaments are detected in [1] using a ref-

Victoria Yu. Salamatova, Sechenov University, Moscow 119991, Russia; Moscow Institute of Physics and Technology, Dolgoprydny 141701, Russia
Alexandra S. Yurova, Sechenov University, Moscow 119991, Russia
***Corresponding author: Yuri V. Vassilevski,** Sechenov University, Moscow 119991, Russia; Moscow Institute of Physics and Technology, Dolgoprydny 141701, Russia; Marchuk Institute of Numerical Mathematics, Russian Academy of Sciences, Moscow 119333, Russia. E-mail: yuri.vassilevski@gmail.com
Lin Wang, Shenzhen Institutes of Advanced Technology, Shenzhen 518055, China

erence registration atlas and a patient-specific affine transformation. The latter is based on virtual palpation, positioning of anatomical points over 3D visualization of CT data. We propose an alternative approach for automatic segmentation of knee bones and detection of origins and insertions for tendons and ligaments. The approach is based on anatomical features on the CT images of bones and landmarks of tendons/ligaments attachments. It provides a tool for the design of patient-specific geometrical knee models, which will be the cornerstone of our future biomechanical knee model.

The rest of the paper is organized as follows. In Section 1 we motivate the use of CT rather than MRI medical images. In Section 2 we present automatic bone segmentation algorithm whereas in Section 3 we address basics for detection of tendons/ligaments origin and insertions. In Section 4 we give an illustrative example for a produced geometrical model.

1 CT and MRI images of knees

Computed tomography (CT) and magnetic resonance imaging (MRI) are non-invasive imaging techniques, which are most commonly used for knee examination in clinical practice. In contrast to CT, MRI modalities provide better resolution of soft tissues and do not expose patients to ionizing radiation. These advantages determine wider use of MRI in comparison with CT, despite of longer acquisition time. MRI is more appropriate technique for clinical examination of knees, since it performs good visualization of ligaments, tendons, cartilages and muscles. On the other hand, automatic segmentation of MRI scans is hampered by the following reasons:

— intensity ranges of the different anatomical structures have intersections;
— appearance of anatomical structures on the MRI images depends on the scanning process, which may vary for different examinations;
— parts of the MRI images may be shaded due to non-uniformity of the magnetic field generated during the examination;
— variability of intensities within the same anatomical structure is typical for MRI images.

As a result, intensity-based segmentation algorithms are not applicable to sustainable segmentation of MRI images. Implementation of the atlas-based or machine learning-based methods is complicated due to lack of available segmented knee datasets. These observations motivate us to use CT images for automatic segmentation of patient's knees.

One can specify four bones making up the knee: thigh bone (*femur*), shinbone (*tibia*), calf bone (*fibula*), kneecap (*patella*). Bones are interconnected and stabilized by ligaments, tough and fibrous tissues. There are five major ligaments associated with the knee joint: the patellar ligament, the medial and lateral collateral ligaments and the anterior and posterior cruciate ligaments [4]. Tendons (represented by a soft tissue) connect a bone and a muscle and provide additional stability to the joint. In general, the knee joint has more than twenty tendons. The exact number of tendons to be detected depends on muscles taken into account in the computational model. The basic knee model [2] involves the following muscles: the quadriceps (vastus medialis, vastus intermedius, vastus lateralis, rectus femoris), the hamstrings (biceps femoris long head, biceps femoris short head, semitendinosus, semimembranosus), and the gastrocnemius (medial head, lateral head).

A segmented 3D CT image forms a 3D geometric model of the four bones, cartilage and positions of tendons and ligaments attachment which is the basis of a personalized biomechanical model of the joint.

2 Bones segmentation algorithm

From image processing view point, a bone is composed of two parts: the outer layer, or the cortical (hard) bone, and the inner part, or the cancellous (trabecular, spongy) bone. The cortical bone can be segmented

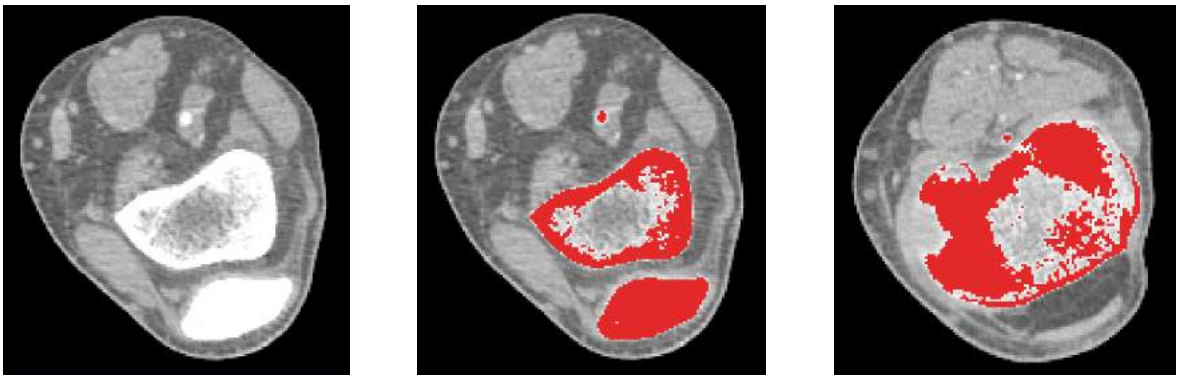

(a) (b) (c)

Fig. 1: Transversal slice of a CT scan (a) and cortical bone segmentation using intensity range [200; 2000] HU for thresholding: continuous contour (b), discontinuous contour (c)

automatically with the use of known threshold values [3, 8]. The outer surface of the cortical bone is assumed to define the bone boundary. However, sometimes the cortical bone thickness may be lower than CT resolution and the outer surface is not a closed surface. Some studies reveal a consistent decrease of cortical thickness with age, that makes the problem of bone boundary detection to be actual for elderly patients. At the same time, the intensity range of the cancellous bones overlaps the intensity ranges of surrounding connective tissue and muscles [8], therefore its threshold-based segmentation becomes impossible. Since the outer surface of the cortical bone represented by its segmentation may contain discontinuities, one can not use the 3D hole-filling algorithm [6] for the cancellous bone segmentation due to possible segmentation leaks into the exterior of the bone. Figure 1 illustrates the above observation for a CT scan of a knee and its continuous and discontinuous threshold-based segmentations on different transversal slices.

We propose Algorithm 1 for knee bones segmentation which alleviates these obstacles. The algorithm starts from the threshold-based initial segmentation of each knee bone, selects the four largest components of the cortical bone representing the four bones of the knee, passes through all 2D slices in transversal, sagittal, and coronal planes and analyzes the background of each slice. If the background has at least two connected components, the other than the largest component of the background belong to the cancellous bones and are segmented by appropriate bone labels. If the contours of the cortical bones are open in a 2D slice and the background has only one connected component, this slice is not processed.

Possible remaining holes in the produced mask are closed by 3D morphological operations, dilation followed by erosion. The example of bone segmentation is demonstrated in Fig.2.

Algorithm 1. Segmentation of bones in a 3D CT image of a knee.

```
1: Segment the cortical bone using thresholding and form the current mask
2: Find connected components of the mask and select four largest components
3: for all the components do
4:     for transversal, sagittal, coronal planes do
5:         for all 2D slices parallel to the current plane do
6:             Find connected components of the background in the 2D slice
7:             Remove the largest connected component
8:             Add the remaining components to the current mask with appropriate labels
9:         end for
10:    end for
11: end for
```

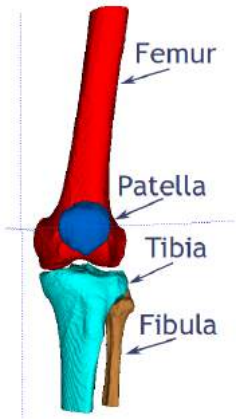

Fig. 2: Segmented bones of a knee joint.

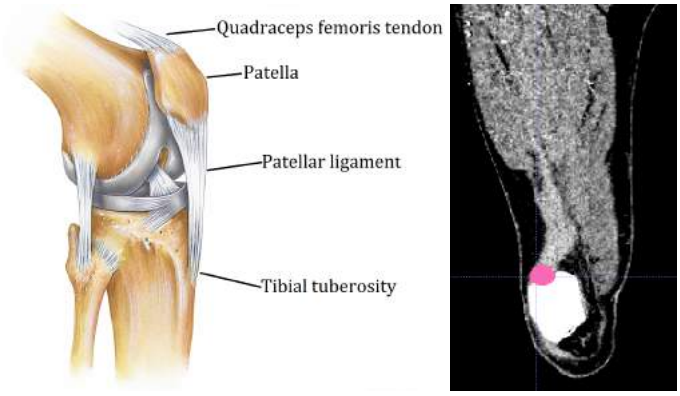

(a) (b)

Fig. 3: Quadriceps femoris tendon and patellar ligament (a); site of tendon attachment on the CT scan (b).

3 Basics for detection of tendons and ligaments attachment

We suggest to estimate virtual landmarks of tendons and ligaments attachment sites using algorithms based on anatomical features and anatomical arrangements. Namely, a tubercle of bone (tuberosity) that is an eminence on the bone surface, often serves as an attachment point for a tendon or a ligament. Sometimes tendon attachment point is associated with a depression in the vicinity of tuberosity (e.g. pes anserinus). Sometimes tendon (ligament) attachment point is associated with a depression on a bone (e.g. attachment of lateral collateral ligament to the femur). Site points near epicondyles and condyles can be traced using analysis of the bone shape and the number of connected components on axial slices of bone segmentation. When the bone surface does not contain any distinguishing tubercles or features, we analyze the CT-intensity gradient along the bone axis (z-axis hereinafter).

To illustrate the ideas of our algorithms, we consider quadriceps femoris tendon and patellar ligament that is the continuation of the quadriceps femoris tendon below the patella up to tibial tuberosity (Fig. 3a). Site of tendon attachment is the upper part of patella, so we can formalize this anatomical arrangement in the following way. We find the patella as the smallest connected component from all bones and dilate our region of interest. To reduce noise impact, we split initial set of CT images into cubes with the size $3\times3\times3$ voxels and replace all voxel intensities within each cube to the mean intensity value over the cube. Then we find voxels with maximum and minimum z-coordinate, compute z-distance $d = z_{\max} - z_{\min}$ between them, and set the tendon attachment as the $3\times3\times3$ cube with maximum intensity value and voxels with $z \in [z_{\max} - d/6; z_{\max}]$, see Fig. 3b.

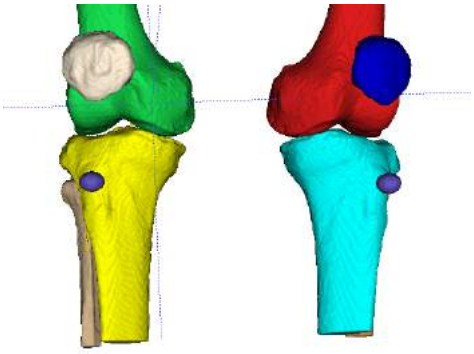

Fig. 4: Tibial tuberosity (purple points).

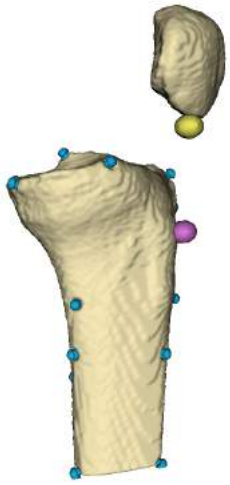

Fig. 5: The lowest patella point (yellow), tibial tuberosity (pink), other tibia tuberosities (blue).

The site of patellar ligament insertion is the tibial tuberosity. Tibial tuberosity is one of bone tubercles which are defined as sites of local maxima of the Gaussian curvature of the bone boundary. The bone boundary is assumed to be given by a triangulated surface mesh. Algorithm 2 defines the general way of detection of the tendons/ligaments attachments.

To identify tibial tuberosity automatically among all detected tubercles, one can take into account the following anatomical peculiarity: patellar ligament is the continuation of the quadriceps femoris tendon below the patella (see Fig. 3). The lowest point of patella and tibial tuberosity are connected with the patellar ligament which is assumed to be approximately colinear to the z-axis as demonstrated in Fig. 4. This anatomical knowledge helps us to find tibial tuberosity. First, we find a point P with coordinates (P_x, P_y, P_z) in patella with the minimal z-coordinate (Fig. 5, yellow point). Second, among all tibial tubercles T_i with coordinates (T_{ix}, T_{iy}, T_{iz}) generated by Algorithm 2 (Fig.5, blue and pink points), we find $\operatorname{argmin}\{(P_x - T_{ix})^2 + (P_y - T_{iy})^2\}$ represented by the pink point in Fig. 5.

Algorithm 2. Tubercles detection on boundaries of segmented knee bones.

1: Generate a surface triangular mesh of the segmented bones
2: Find the Gaussian curvature at each mesh node
3: Detect tubercles as local maxima of the curvature
4: Select tubercles corresponding to sites of tendons/ligaments attachment

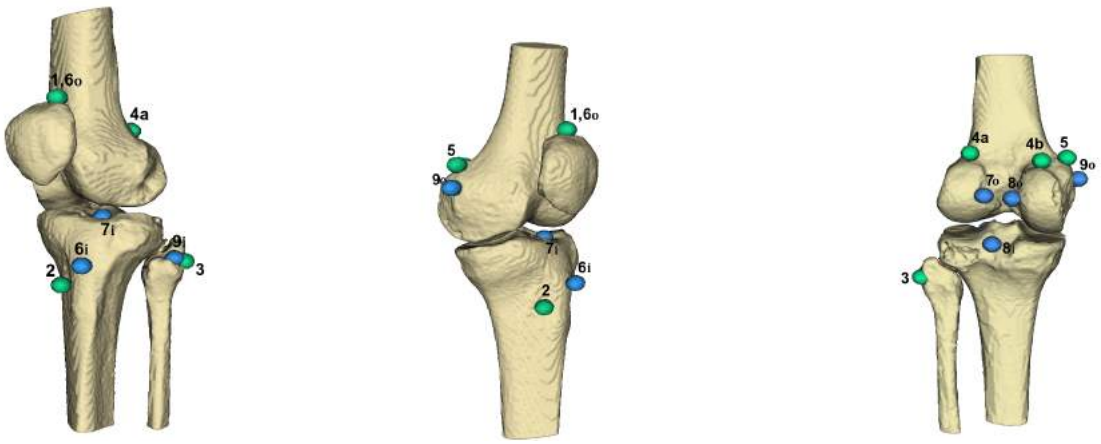

Fig. 6: Tendons (green points): 1 — quadriceps femoris, 2 — semitendinosus, 3 — biceps femoris, 4 — gastrocnemius (a — lateral head, b — medial head), 5 — adductor longus, Ligaments (blue points; subscript 'o' for origin, 'i' for insertion: 6 (6o-6i) — patellar ligament, 7 (7o-7i) — anterior cruciate ligament, 8 (8o-8i) — posterior cruciate ligament, 9 (9o-9i) — lateral (fibular) collateral ligament.

4 Example

We apply the proposed algorithms to a dataset of four human knees. We were able to identify almost all tendon and ligament attachments required by the basic human knee model except tibial collateral ligament and semimembranosus muscle. One of the obtained geometrical models is shown in Fig. 6. Points 1 and 6 coincide in Fig. 6 since the attachment of the quadriceps femoris tendon and the origin of the patellar ligament coincide. Detected origins and insertions define ligaments, e.g., the segment 8o-8i defines the posterior cruciate ligament. The site of tendon attachment, e.g., point 1, can be used as the loading center for a muscle action. These data form the geometrical basis of the future biomechanical knee model. Full description of the algorithms and analysis of the results will be presented elsewhere.

5 Conclusions

We proposed anatomy-based algorithms for automatic generation of personalized geometrical models for human knees. The main limitations of our approach are given by anatomical abnormalities of knee bones and representation of tendons/ligaments attachment site by a point rather than a patch. These limitations will be alleviated in the future work.

Funding: The work was supported in part by the world-class research center 'Moscow Center for Fundamental and Applied Mathematics', RFBR grant 17-01-00886, the 2019 International Collaboration Special Plan, Chinese Academy of Sciences, grants of Guangdong Province, China, 2018A030313065 and Shenzhen, China, JCYJ20170818163445670.

References

[1] D. Ascani, C. Mazzà, A. de Lollis, M. Bernardoni, and M. Viceconti, A procedure to estimate the origins and the insertions of the knee ligaments from computed tomography images. *J. Biomechanics* **48** (2015), No. 2, 233–237.

[2] T. F. Besier, M. Fredericson, G. E. Gold, G. S. Beaupré, and S. L. Delp, Knee muscle forces during walking and running in patellofemoral pain patients and pain-free controls. *J. Biomechanics* **42** (2009), No. 7, 898–905.

[3] J. de Carvalho Felinto et al., Automatic segmentation and quantification of thigh tissues in CT images. In: *Computational Science and Its Applications – ICCSA 2018. Lecture Notes in Computer Science, vol 10960* (Eds. O. Gervasi et al). Springer, Cham, 2018, pp. 261–276.
[4] R. L. Drake, A. W. Wayne Vogl, and A. W. M. Mitchell, *Gray's Anatomy for Students*. Fourth Edition, Elsevier.
[5] B. E. Gage, N. M. McIlvain, C. L. Collins, S. K. Fields, and R. D. Comstock, Epidemiology of 6.6 million knee injuries presenting to United States emergency departments from 1999 through 2008. *Academic Emergency Medicine* **19** (2012), No. 4, 378–385.
[6] R. C. Gonzalez and R. E. Woods, *Digital Image Processing*, 2nd Edition. Prentice Hall, 1992.
[7] *Handbook of Biomedical Image Analysis* (Eds. J. S. Suri, D. L. Wilson, and S. Laxminarayan). Springer US, Boston, 2005.
[8] M. Hofer, *CT Teaching Manual: A Systematic Approach to CT Reading*. Thieme, 2010.
[9] J. C. Küpper, B. Loitz-Ramage, D. T. Corr, D. A. Hart, and J. L. Ronsky, Measuring knee joint laxity: a review of applicable models and the need for new approaches to minimize variability. *Clinical Biomechanics* **22** (2007), No. 1, 1–13.